

Observation of Long-Range Intensity Correlation in the Transport of Coherent Light through a Random Medium

M. P. van Albada,⁽¹⁾ J. F. de Boer,⁽¹⁾ and A. Lagendijk^(1,2)

⁽¹⁾*Natuurkundig Laboratorium, Universiteit van Amsterdam, Valckenierstraat 65,
1018XE Amsterdam, The Netherlands*

⁽²⁾*Stichting voor Fundamenteel Onderzoek der Materie—Institute for Atomic and Molecular Physics,
Kruislaan 407, 1089SJ Amsterdam, The Netherlands*

(Received 23 October 1989)

We have measured the correlation in frequency-dependent intensity fluctuations in the total transmission through random dielectric samples, using visible light in a (essentially) plane-wave geometry. The correlation function, of which the width at half maximum is proportional to L^{-2} (L is the thickness of the sample), decays as $(\Delta\omega)^{-1/2}$. This constitutes the experimental proof for the buildup of long-range intensity correlations in the propagation of classical waves by multiple scattering.

PACS numbers: 42.20.-y

In recent years it has become clear that the multiple elastic scattering of coherent waves by disordered media does not merely scramble the incident wave in a random manner, but that the apparent randomness of the scattered wave conceals a number of intriguing interference effects. Localization (weak) of electrons, resulting from interference between time-reversed pairs of waves (waves that propagate in opposite directions along the same sequence of scatterers) has been known for some time.¹ More recently enhanced backscattering of light due to weak localization was observed.² Weak localization, however, is not the only effect of interference upon the scattered intensity pattern. The conductance g of a disordered metallic sample in a varying magnetic field exhibits field-dependent fluctuations, known as “universal” conductance fluctuations (UCF) because it has been found that the variance of g is approximately e^2/h , (essentially) independent of sample parameters.³ The conductance fluctuations may be explained in terms of field-induced changes in the relative phases, and hence in the interference, of waves propagating along different Feynman paths that have scattering centers in common. One may expect the same type of interference to occur in classical wave propagation by multiple scattering, where relative phase changes could be induced by, e.g., varying the wavelength. The present work deals with effects of this interference in light transport through a random dielectric medium.

We first present a model to describe the system under study. Consider a waveguide, part of which is occupied by a random sample. The waves that interact with the sample are superpositions of propagating eigenmodes, and these eigenmodes function as channels through which current is coupled into—or out of—the sample. In the case of a sample in free space (e.g., a locally illuminated slab of random dielectric material) no discrete modes exist. Here, a channel is a solid angle containing one coherence area or—in practical terms—having the size of a speckle spot. The number of modes (or chan-

nels) is given by $N = 2\pi A/\lambda^2$, where A is the cross section of the waveguide or the illuminated area of the slab. Let $t_{\alpha\beta}$ be an amplitude transmission coefficient giving the amplitude in outgoing channel β that is due to the amplitude in incoming channel α , and let $T_{\alpha\beta} = |t_{\alpha\beta}|^2$. Current conservation imposes correlations among the $T_{\alpha\beta}$.

At this stage it is useful to note that, while the interference effects that occur in quantum and classical wave transport may well be equivalent, the parameters that are accessible to direct observation in, e.g., a conduction experiment and a light-scattering experiment are not: In a conductance experiment the electrons enter or leave the sample through its interfaces with perfectly conducting leads, and are reflected by the lateral boundaries. Only the total current through the sample can be measured, under conditions where mutually uncorrelated signals are present in all input channels. The conductance (the object that exhibits UCF) depends on all N^2 coefficients $t_{\alpha\beta}$. To directly observe “UCF” in an optical experiment one would need a sample with perfectly reflecting lateral boundaries of which one interface is illuminated with quasimonochromatic diffuse light. The reflectivity condition is difficult to meet. In a light-scattering experiment one may, on the other hand, exit, for instance, just one input channel, or study spatial correlations in the scattered intensity. Such experiments provide information on intensity correlations that cannot be obtained from measuring the electronic conductivity.

Intensity-intensity correlations that occur in diffuse wave transport have recently raised a lot of theoretical interest.⁴⁻¹⁰ It has been predicted that, in addition to a short-range correlation, long-range correlations exist, that build up when waves propagating along different “light paths” interfere in regions of the sample where sections of these paths happen to coincide. The picture that has emerged from theory is the following: The spatial correlation $C_{\alpha\beta\alpha'\beta'}$ (the ensemble average $\langle \delta T_{\alpha\beta} \times \delta T_{\alpha'\beta'} \rangle$) is a sum of three terms, $C^{(1)}$, $C^{(2)}$, and $C^{(3)}$,

describing short-, long-, and infinite-range correlations, respectively. The term $C^{(n)}$ has the form $C_0^{(n)} \times F_n(\alpha, \alpha', \beta, \beta')$, where $C_0^{(n)}$ is 1, g^{-1} , or g^{-2} , respectively ($g = Nl/L$, the “conductance” of the sample, where l is the mean free path), and F_n is a form function that depends on the relative orientation of the input channels and the output channels. $C^{(1)}$ contributes only for $\Delta q_\alpha = \Delta q_\beta$ (“memory effect”) and F_1 decays as $(\Delta qL)^2 / \sinh^2(\Delta qL)$ (Δq is the transverse momentum change). $C^{(2)}$ contributes essentially if either $\Delta q_\alpha = 0$ or $\Delta q_\beta = 0$. In a “one-channel-in” geometry it will be present among all transmission channels, and therefore show in the total transmission. $C^{(3)}$ contributes uniformly for all Δq_α and Δq_β .

$C^{(1)}$ -type^{5,10} and $C^{(2)}$ -type¹⁰ correlations in the frequency domain have been calculated as well: Genack⁵ calculated the short-range correlation that we will write here as

$$C^{(1)}(\Delta\omega, L) = \langle \delta T_{\alpha\beta}(\omega) \delta T_{\alpha\beta}(\omega') \rangle = F_1(\Delta\omega, L), \quad (1)$$

where

$$F_1(\Delta\omega, L) = x^2 / [\cosh(2x) - \cos(2x)],$$

with $x = (\Delta\omega/D)^{1/2}L$, and $D = vl/3$. Pnini and Shapiro¹⁰ calculated the long-range correlation

$$\left\langle \delta \sum_{\beta} T_{\alpha\beta}(\omega) \delta \sum_{\beta'} T_{\alpha\beta'}(\omega') \right\rangle = (l/9NL) F_2(\Delta\omega, L), \quad (2)$$

with

$$F_2(\Delta\omega, L) = \frac{3}{2} x^{-1} \frac{\sinh(2x) - \sin(2x)}{\cosh(2x) - \cos(2x)}.$$

[From Eq. (2), and using Pnini’s expression for $\langle T \rangle$, it follows that $\langle \delta T^2 \rangle / \langle T \rangle^2 = L/Nl = g^{-1}$.]

Experimentally, the form function $F_1(\Delta\omega, L)$ has been measured⁵ and very good agreement was found with theory. The conservation of transverse momentum change or memory effect as predicted by Feng *et al.*⁹ has been experimentally confirmed by Freund and Rosenbluh.¹¹ Garcia and Genack¹² measured $C_{\alpha\alpha'\beta\beta'}(\Delta\omega, L)$ in a microwave experiment, using samples of very limited transverse dimensions (i.e., small g) with reflecting lateral walls. For samples with large L , they could follow the decay into the range of $\Delta\omega$ values for which $g^{-1}F_2 > F_1$ as demonstrated by a crossover from exponential (F_1) to power-law (F_2) decay.

This paper reports on the first experimental study of the complete form function $F_2(\Delta\omega, L)$, and its comparison to the function $F_1(\Delta\omega, L)$, that depends on the same parameters. We obtained small “samples” by focusing a laser beam upon a slab of random dielectric material, and studied the correlation functions $\langle \delta T_{\alpha\beta}(\omega) \times \delta T_{\alpha\beta}(\omega') \rangle_\omega$ and $\langle \delta \sum_{\beta} T_{\alpha\beta}(\omega) \delta \sum_{\beta'} T_{\alpha\beta'}(\omega') \rangle_\omega$ for different values of L , using TiO₂-air samples and visible light. The form function F_2 was obtained dividing the latter correlation function by its autocorrelate.

The setup as used for total transmission measurements is shown schematically in Fig. 1. A “coherent radiation”

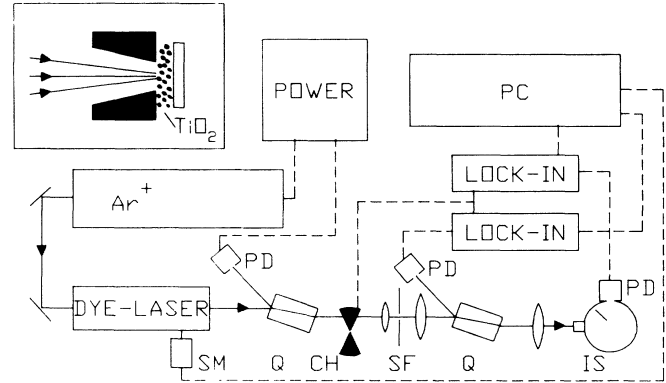


FIG. 1. Experimental setup for the recording of fluctuations in the total transmission. SM, stepper motor; Q, quartz beam splitter; CH, chopper; SF, spatial filter; IS, integrating sphere. Inset: Inset as fitted in port of integrating sphere, carrying a sample on transparent supporting material.

590 dye laser was used as a source, and its frequency was varied by driving the birefringent filter under computer control. The beam was chopped, filtered, expanded slightly, and then focused onto the slab. The “sample size” could be varied by moving the focusing lens with respect to the slab. By using a ratio technique, the fluctuations under study were separated from fluctuations in the source power. The effect of possible slight nonlinearities of the detectors was minimized by maintaining the output power of the source essentially constant throughout the scans, using a feedback circuit coupled to the power supply of the pump laser. A slow drift in the fluctuation pattern, resulting from wavelength dependence of the properties of the beam splitter, average transmission of the sample, and absorption by the sample and integrating sphere was eliminated, dividing by background curves recorded with an unfocused probe beam. In the “one-channel-out” (F_1) experiments, the integrating detector was replaced by a photomultiplier, fitted with a polarizer and a pinhole. Corrections were made for the differing response curves of the probe and reference detectors. Thin samples were studied with the dye laser operating in the broadband mode; for samples thicker than approximately 30 μm , it was used in the single-frequency mode.

Samples were prepared by spreading suspensions of TiO₂ pigment on a transparent substrate. After evaporation of the liquid, the sample thickness was determined microscopically. Several (5–20) intensity patterns were recorded per sample (and per type of scan). The correlation function $\langle \delta I(\omega) \delta I(\omega') \rangle$ was calculated for every individual scan, and the resulting curves were averaged.

Figure 2 shows the shape of the F_1 form function as determined for a $L = 17 \mu\text{m}$ sample. The solid curve was calculated according to Eq. (1) using $D = 10.7 \text{ m}^2 \text{ s}^{-1}$. (Assuming a value of $\approx 1.6 \times 10^8 \text{ m s}^{-1}$ for the velocity of light in the medium, we find from $D = vl/3$ that

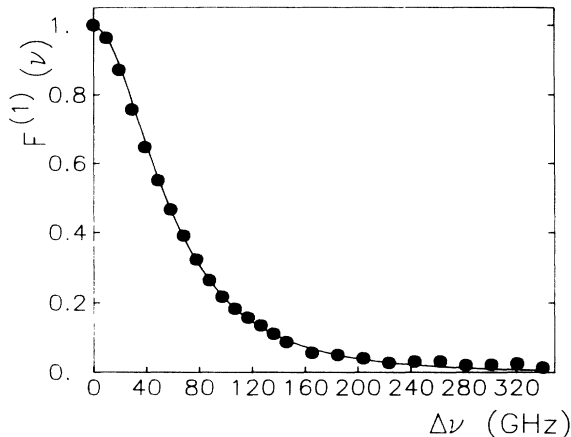


FIG. 2. Comparison of the form function $F_1(\Delta\omega, L)$ as calculated using $D=10.7 \text{ m}^2\text{s}^{-1}$ (solid curve) with the experimental data (solid circles) for a TiO_2 -air sample with $L=17 \mu\text{m}$.

$l \approx 200 \text{ nm}$.) The calculated $F_1(\Delta\omega, L)$ is in excellent agreement with experiment. The diffusion constant D can also be calculated from the width of the cone of enhanced backscattering. If internal reflection¹³ at the sample-air interface is neglected, a value of about $17 \text{ m}^2\text{s}^{-1}$ is obtained. Correction for this internal reflection will lead to a value that is considerably lower, but to our estimate not lower than about $8 \text{ m}^2\text{s}^{-1}$. Thus, the value of D that fits Eq. (1) to the data is consistent with results from enhanced backscattering experiments.

Figure 3 shows the F_2 form function as measured for the same $17\text{-}\mu\text{m}$ sample. The dashed curve, calculated according to Eq. (2), corresponds to the prediction for a plane-wave geometry. Since $C^{(2)}$ is proportional to g^{-1} , F_2 cannot be measured in a plane-wave geometry: The transverse dimensions of the sample must be made small for the fluctuations in $\sum_{\beta} T_{\alpha\beta}$ to show above the level of instrumental noise. A small illuminated area, however, implies that rapidly dephasing contributions will be underrepresented, and hence the decay of the correlation with increasing $\Delta\omega$ will be slower. Indeed we found that the width of the correlation function decreases upon increasing the size of the illuminated spot. The results presented in Fig. 3 were obtained using a Gaussian spot with a diameter that was considerably larger than the sample thickness, and $g \approx 1000$. As the signal-to-noise ratio did not permit a further increase of the spot size, we do not know whether such an increase would further reduce the width of F_2 . It appears that Eq. (2) may be fitted to the experimental data by multiplying the argument of F_2 by a factor < 1 . The solid curve in Fig. 3 was obtained in this way, using 0.77 as a factor. From our present data no firm conclusion can be reached as to whether the factor is geometrical, related to absorption, or an inherent one that should emerge in an improved plane-wave-limit theory.

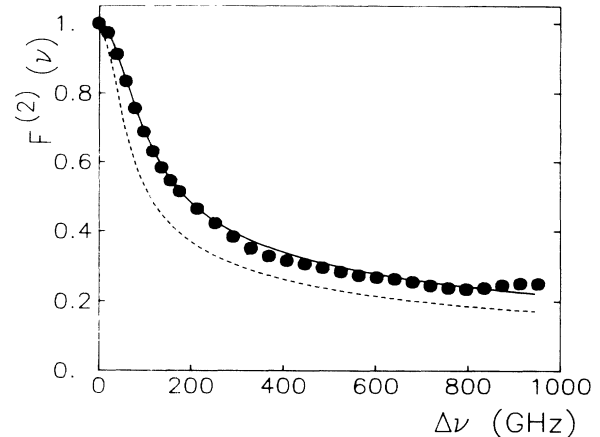


FIG. 3. Comparison of the form function $F_2(\Delta\omega, L)$ with the experimental data (solid circles) for a $L=17 \mu\text{m}$ TiO_2 -air sample. Dashed curve, theoretical curve for plane-wave geometry; solid curve, argument of plane-wave F_2 multiplied by an empirical factor (see text).

Log-log plots of $F_2(\Delta\omega, L)$ vs $\Delta\omega$ yield essentially straight lines with slopes in the range 0.5 ± 0.1 . At the high- $\Delta\omega$ side, structure appears that is due to the limited range of the individual scans. By averaging more curves, the length of the straight part of the curve can be extended. Figure 4 shows the average of four correlation functions as measured using a $35\text{-}\mu\text{m}$ sample. It clearly shows the $(\Delta\omega)^{-1/2}$ decay.

Figure 5 shows the width of half-height of both F_1 and F_2 as a function of the sample thickness. The L^{-2} dependence is evident in both cases. The proportion $\Delta\omega_{1/2}^{(2)}/\Delta\omega_{1/2}^{(1)}$ appears to be independent of L , and (at least in our experimental geometry) is about 3.2 . For a plane-wave geometry, Ref. 10 predicts it to be 2 . We note that the width of F_1 , which depends exclusively on the distribution of photon flight times, is not affected by

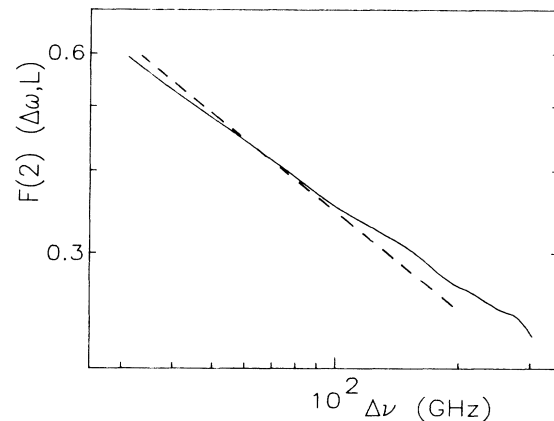


FIG. 4. Solid line, log-log plot of $F_2(\Delta\omega, L)$ vs $\Delta\omega$ as measured for a $35\text{-}\mu\text{m}$ sample; dashed line, the $(\Delta\omega)^{-1/2}$ decay.

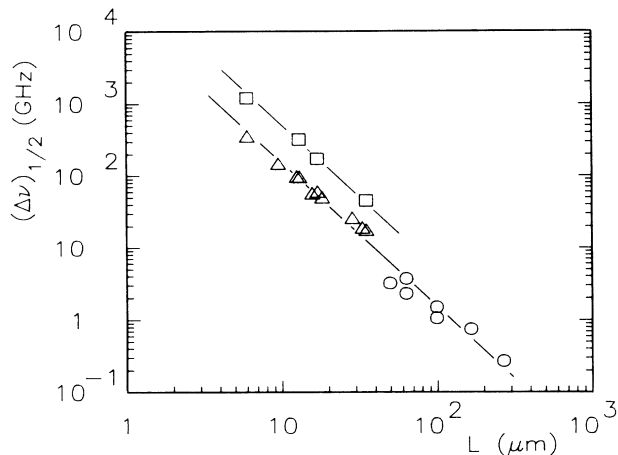


FIG. 5. Width at half maximum of the form functions $F_1(\Delta\omega, L)$ and $F_2(\Delta\omega, L)$. F_1 , measured with the dye laser in broadband mode (Δ); F_1 , measured with the dye laser in a single-frequency mode (\circ); and F_2 , measured with the dye laser in broadband mode (\square).

the experimental geometry.

A more detailed study of both $C^{(2)}(\Delta\omega, L)$ and $C^{(2)}(\Delta qL)$ is now underway.

Summarizing, we have experimentally proved that long-range intensity correlations build up in the propagation of coherent light through multiple scattering, by demonstrating that when light is fed into essentially one input channel, the correlation function for the frequency-dependent fluctuations that are observed in the total transmission decays with $(\Delta\omega)^{-1/2}$.

The authors would like to thank P. de Vries and M. B. van der Mark for helpful discussions. This work was supported in part by the "Stichting voor Fundamenteel

Onderzoek der Materie (FOM)," which is a part of the "Nederlandse Organisatie voor Wetenschappelijk Onderzoek (NWO)."

¹G. Bergman, Phys. Rep. **107**, 1 (1984); *Anderson Localization*, edited by T. Ando and H. Fukuyama (Springer-Verlag, Berlin, 1988).

²Y. Kuga and A. Ishimaru, J. Opt. Soc. Am. A **1**, 831 (1984); M. P. van Albada and A. Lagendijk, Phys. Rev. Lett. **55**, 2692 (1985); P. E. Wolf and G. Maret, Phys. Rev. Lett. **55**, 2696 (1985). For recent reviews, see S. John, Comments Condens. Matter Phys. **14**, 193 (1988); "Classical Wave Localization," edited by P. Sheng (World Scientific, Singapore, to be published).

³C. P. Umbach, S. Washburn, R. B. Laibowitz, and R. A. Webb, Phys. Rev. B **30**, 4048 (1984).

⁴B. Shapiro, Phys. Rev. Lett. **57**, 2168 (1986).

⁵A. Z. Genack, Phys. Rev. Lett. **58**, 2043 (1987); A. Z. Genack and J. M. Drake (unpublished).

⁶B. Z. Spivak and A. Yu. Zyuzin, Solid State Commun. **65**, 311 (1988); A. Yu. Zyuzin and B. Z. Spivak, Zh. Eksp. Teor. Fiz. **93**, 994 (1987) [Sov. Phys. JETP **66**, 560 (1987)].

⁷M. J. Stephen and G. Cwilich, Phys. Rev. Lett. **59**, 285 (1988).

⁸P. A. Mello, E. Akkermans, and B. Shapiro, Phys. Rev. Lett. **61**, 459 (1988).

⁹S. Feng, C. Kane, P. A. Lee, and A. D. Stone, Phys. Rev. Lett. **61**, 834 (1988).

¹⁰R. Pnini and B. Shapiro, Phys. Rev. B **39**, 6986 (1989).

¹¹I. Freund and M. Rosenbluh, Phys. Rev. Lett. **61**, 2328 (1988).

¹²N. Garcia and A. Z. Genack, Phys. Rev. Lett. **63**, 1678 (1989).

¹³A. Lagendijk, R. Vreeker, and P. de Vries, Phys. Lett. A **136**, 81 (1989).